Co-published by
Institute of Fluid-Flow Machinery
Polish Academy of Sciences
Committee on Thermodynamics and Combustion
Polish Academy of Sciences

Copyright©2025 by the Authors under licence CC BY-NC-ND 4.0

http://www.imp.gda.pl/archives-of-thermodynamics/

Experimental and theoretical investigation of thermally insulated roof slabs

Anil Kumar Dixit[a], Manmatha Kumar Roul[b*], Bikasha Chandra Panda[c], Prajna Priyadarsini Roul[b], Sibakanta Sahu[b], Prateek Debadarsi Roul[c], Saipada B.B.P.J. Sahu[d]

[a]Bhadrak Institute of Engineering & Technology, Bhadrak-756113, Odisha, India
[b]GITA Autonomous College, Bhubaneswar-752054, Odisha, India
[c]Indira Gandhi Institute of Technology, Sarang-759146, Odisha, India
[d]National Institute of Technology, Rourkela-769008, Odisha, India
*Corresponding author email: mkroul@gmail.com

Received: 10.06.2025; revised:28.07.2025; accepted: 03.08.2025

Abstract

In this analysis, thermal performance of building roof elements subjected to periodic changes in temperature at a roof top was examined with and without insulating materials. The objective of this analysis is to reduce energy consumption and prevent heat flow through roofs by using various insulating materials on the roof slab. It aims to compare the thermal performance of roof slabs with and without insulation under different atmospheric temperature conditions. Further, the study seeks to accurately predict the roof bottom temperature using optimisation techniques in order to minimise experimental cost and time. Nine identical rooms were constructed and eight roofs were retrofitted with different insulating materials such as coconut shell, fly ash, Jhama brick bats, rice husks, glass fibre, rubber sheet, earthen pots and asbestos sheets. The roof of one room was kept untreated and was considered as a reference. The thermal behaviour of every innovative roof slab was analysed. Among the eight insulating materials considered in this study, the performance of the roof slab with fiberglass was found to be the best. Roof slab with fiberglass could provide temperature reduction in the room of about 6.17°C, whereas roof slab with earthen pot could provide temperature reduction in the room of 2.27°C. The time lag between the maximum roof top temperature and maximum room temperature was found to be maximum in the case of roof slab with fiberglass and minimum in the case of roof slab with earthen pot. The time lag between the maximum roof top temperature and maximum room temperature is 4 hours for roof slab with fiberglass. The variation of roof bottom temperature was predicted by five optimisation techniques such as cuckoo search, bacterial colony optimisation, group search optimisation, social spider optimisation and genetic algorithm. It was observed that the social spider optimisation technique predicted the temperature accurately and the error between the measured and predicted temperature values was minimum compared to the other optimisation techniques.

Keywords: Thermal insulation; Insulating materials; Thermal performance; Optimisation techniques; Time lag.

Vol. 46(2025), No. 4, 187–199; doi: 10.24425/ather.2025.156849

Cite this manuscript as: Dixit, A.K., Roul, M.K., Panda, B.C., Roul, P.P., Sahu, S., Roul, P.D., & Sahu, S.B.B.P.J. (2025). Experimental and theoretical investigation of thermally insulated roof slabs. *Archives of Thermodynamics*, 46(4), 187–199.

1. Introduction

Construction of buildings is one of the oldest established activities since the creation of human civilisation [1]. Man has transformed a lot in the construction of houses, right from caves to huts and from huts to reinforced cement concrete (RCC) structures. RCC slabs are commonly used in roofs, walls and floors of buildings and bridges. The temperature inside houses with RCC roof slabs is required to be maintained at the desired level for the comfort of occupants. The application of insulating materials has increa-

Nomenclature

A – surface area, m²
d – thickness of test specimen. m
F – inverse of calorimeter heat transfer coefficient, 1/N
N – heat transfer coefficient of reference calorimeter
Q – heat flux, W/m²
R_s – thermal resistance of the test specimen, m² K/W
R_{int} – interface thermal resistance, m² K/W
T_u – temperature of upper plate, K or °C
T_m – temperature of the middle plate, K or °C
T_l – temperature of bottom heater plate, K or °C
U – overall heat transfer coefficient, W/(m² K)

Greek symbols

λ – thermal conductivity, W/(m·K)
ΔT_s – temperature difference across test sample, K
ΔT_s – temperature difference across reference calorimeter, K

Subscripts and Superscripts

int – interface
l – lower or bottom heater plate
m – middle or test sample interface
r – reference (calorimeter or temperature difference)
s – sample
u – upper plate

Abbreviations and Acronyms

BCO – bacterial colony optimisation
CS – cuckoo search
GA – genetic algorithm
GSO – group search optimisation
HVAC – heating, ventilation and air conditioning
IR – infrared
RCC – reinforced cement concrete
SSO – social spider optimisation

sed appreciably in recent years. One or more of the insulating materials may be provided in the form of a ceiling board in order to maintain thermal comfort inside the room [2].

Rock may be used as material for building walls; wood may be employed to provide roofing support; a ceiling may be provided to reduce temperature inside buildings [3]. It has been a matter of concern for the engineers to design a building that can provide thermal comfort for the occupants [4]. There exist design and structural differences between the developments in the ground-level landscape and rooftop [5]. Lundholm et al. [6] observed that buildings with green roofs use less energy in the summer. They measured the heat flux for extensive green roof systems and determined their dependence on solar radiation, temperature of the substrate and depth of the snow cover. They also verified the connections between vegetation type, snow accumulation and substrate temperature. Considering the rooftop developments, thermal expansion may be caused due to absorption of heat energy in the roof slabs that may lead to cracks in the load-bearing masonry materials [7]. Therefore, a suitable insulation system is required in the roof slabs to overcome this problem [8]. Insulation is very much essential in buildings to shield the building from the inflow of heat from outside during summer and outflow of heat from the building during winter and to attain thermal comfort for its dwellers during warm summers and cold winters [9,10]. Björk and Enochsson [11] investigated the performance and durability of thermal insulation materials under extreme environmental conditions, highlighting their impact on long-term thermal efficiency in building applications.

Gagliano et al. [12] explored the effectiveness of ventilated roofs portrayed by different insulation layers with respect to the air gap. Their results show that the aeration through roofs can decrease heat fluxes considerably in the summer season. Halwatura and Jayasinghe [13] proposed different insulation systems for roof slabs and studied experimentally their performances using small and large-scale models. Jaffal et al. [14] provided a detailed investigation of the impact of a green roof on indoor temperature. With a green roof, the temperature inside the building could be lowered by 2°C in summer, with a significant decrease in the annual requirement of energy. Dong et al. [15] examined the consequence of various factors, such as phase change material thickness, latent heat, radiation intensity, roof slope, absorption coefficient, etc., on the temperature delay, thermal comfort and energy consumption. Dixit et al.[16] used different optimisation techniques, such as bacterial colony optimisation (BCO), cuckoo search (CS) and group search optimisation (GSO) to determine the most favourable weight of the structure.

Numerous studies have been carried out on natural convection heat transfer, providing the scientific basis for experimental and theoretical investigation of thermally insulated roof slabs. Roul and Nayak [19] investigated heat transfer within vertical tubes. Nayak et al. [20−22] presented the enhancement of heat transfer in vertical tube due to internal obstacles. In their work, they considered rings of rectangular cross section as internal obstacles. Sahoo et al. [23−26] employed computational fluid dynamics techniques to analyse heat transfer from pin finned horizontal and vertical plates. Roul and Sahoo [27] investigated the pressure drop through pipes with variable cross sectional area, which is necessary for estimating the power required to pump the fluid through the pipe to create forced draft. Himrane et al. [28] investigated thermal comfort by numerical simulation of natural convection in an enclosed cavity, based on the lattice Boltzmann method, analysing the effects of Rayleigh number (Ra) and oscillation amplitude on temperature distribution and flow behaviour. Their study provides valuable insights into airflow patterns, thermal stratification, and heat transfer characteristics under varying thermal and dynamic conditions. Belenguer et al. [29] experimentally investigated the efficiency of different methods used for reducing energy requirements in homes and achieved a reduction in energy consumption up to 14.6%. Martínez et al. [30] generated computational models to envisage the effectiveness of external walls to provide thermal comfort and validated their model experimentally using waste insulating materials. Chandra et al. [31] introduced an innovative approach to insulate the roof by employing bamboo strips and found the most favourable thickness of insulation layer, which can reduce the maximum temperature at the peak hour with the highest de-

lay in time. Koru [32] investigated some insulation materials and found that the thermal conductivity depends mostly upon density, moisture content, size and configuration of pores and environmental conditions. Alyami [33] employed a simulation tool to determine various climatic zones and observed that climatic conditions affect the performance of buildings as regards energy efficiency. Kumar et al. [34] estimated the economic viability and environmental affability of the thickness of insulation used for ducts in heating, ventilation and air conditioning (HVAC) systems to minimise the energy loss, taking into account different insulating materials. Alnahhal et al. [35] studied both computationally and analytically the insulation in walls and roofs with air cavities for variable aspect ratios and found the optimum aspect ratio for providing thermal insulation to minimise energy consumption in buildings. Alhefnawi and Abdu-Allah Al-Qahtany [36] observed that the geometry, orientation, material and type of construction of buildings affect the heat transfer to the buildings through the walls and roofs. They also examined the effectiveness of an air gap as a thermal insulator to reduce the energy requirement for air conditioning purposes. Sassine et al. [37] used hollow blocks with various void ratios so as to augment the thermal resistance of the wall and decrease the heat transfer to the room.

Thermal insulation of roof slabs plays an important role in improving the comfort of inhabitants by dropping the indoor air temperature. Heat transfer through the roof decreases significantly by providing thermal insulation under or on the roof slab. In the present analysis, the thermal performance of building roof elements subjected to periodic changes in temperature at the roof top was examined, with and without insulating materials. Nine identical rooms were constructed and eight roofs were outfitted with different insulating materials, such as coconut shell, fly ash, Jhama brick bats, rice husks, fibreglass, rubber sheet with aeration, earthen pots and asbestos chips. The roof of one room was kept untreated (no insulation) and was considered a reference. The thermal behaviour of all innovative roof slabs was analysed. For each room, the experiment examines the room temperature with an insulating material and without an insulating material, along with the roof bottom temperature and roof top temperature, atmospheric temperature and temperature inside the room.

The investigation implies that the roof model with insulating material achieves better performance than the one without insulating material. Thermal insulation reduces the heat flow through the roof, as a result of which the energy requirement of the building can be reduced and the comfort of the occupants can be improved. The variation of the roof bottom temperature was predicted by five optimisation techniques, such as bacterial colony optimisation (BCO), cuckoo search (CS), group search optimisation (GSO), genetic algorithm (GA) and social spider optimisation (SSO). To minimise experimental cost and time, these optimisation techniques can be used to predict the roof bottom temperature when various insulating materials are employed at the top of the roof. The various inputs considered for the theoretical analysis are wall area, thickness, testing temperature and time. The methodology is prepared by taking 80% of the dataset for the training function and utilising the remaining 20% of the dataset to validate the model. In the proposed numerical modelling, the objective function is formulated in agreement with the measured output parameters. The mathematical modelling with optimisation predicts results with minimum error by incorporating the optimal weights. We have effectively employed a number of optimisation techniques to establish the optimal weight of the system and to predict the roof bottom temperature. These mathematical models are found to be time and cost-effective. The MATLAB 2018 software was utilised to implement the complete procedure of different optimisation methods. A total of 285 data were used, out of which 228 were training data.

Objectives and scope of this analysis is to (i) reduce the energy consumption and prevent heat flow through the roofs by using various insulating materials on roof slab, (ii) compare the roof slab with and without insulating materials and determine the thermal performance of roof elements under various atmospheric temperature conditions, and (iii) accurately predict the roof bottom temperature by using different optimisation techniques in order to minimise cost and duration of the experiment.

In contrast to previous studies that examined the effects of singular or limited insulating materials or focused solely on simulation, the present work provides a comprehensive experimental and theoretical investigation of eight different insulating materials, many of which are locally available and environmentally sustainable, installed under real environmental conditions. The study uniquely combines experimental data with advanced optimisation algorithms (BCO, CS, GSO, GA and SSO) to predict roof bottom temperatures with high accuracy. The use of social spider optimisation as a predictive model, in particular, has not been widely reported in this context and demonstrates superior accuracy over traditional methods. This dual approach not only helps in identifying the most effective insulating materials for energy-efficient construction but also presents a cost and time-effective methodology for temperature prediction in thermally insulated roof systems. Therefore, this research significantly contributes to the design of thermally efficient buildings, particularly in hot and humid climates, and fills a gap in the literature by offering both performance comparison and predictive modelling of various insulation strategies.

2. Experimental investigations

Nine identical rooms with internal dimensions of 1m × 1m × 1m were constructed.

The selection of insulating materials in this study was motivated by a combination of factors, including thermal properties, environmental sustainability, cost-effectiveness and local availability. Each material was chosen based on one or more of the following considerations. Coconut shells, rice husks, fly ash, Jhama brick bats and earthen pots are locally available agricultural or industrial by-products, often considered waste materials. Their reuse aligns with sustainable construction practices and helps reduce environmental burdens by promoting waste valorisation. These materials are economically viable, making them suitable for low-cost construction in rural and semi-urban areas. They are widely accessible and affordable, allowing for scalable application in developing regions. Materials like earthen pots

and rice husks have inherent thermal insulation properties due to their porous structure and low thermal conductivity. Fly ash and Jhama brick bats are commonly used in construction fill or waste management and have shown potential in improving thermal mass, thereby contributing to passive cooling when integrated into roofing systems. Glass fibre was selected as a benchmark commercial insulating material due to its established performance in modern construction. Including it allowed for comparison between conventional and unconventional (eco-friendly) alternatives. Rubber sheets and asbestos sheets were selected for their known insulation characteristics and availability as roofing components in various commercial and industrial applications.

By incorporating a diverse range of materials, from natural and agricultural waste to industrial by-products and commercial insulators, the study aims to provide a holistic evaluation of thermal performance and support the selection of sustainable, cost-effective roofing solutions across varied socioeconomic and climatic contexts.

Roof top surface temperatures were measured using a Fluke 62 Max infrared thermometer (which offers single laser targeting for accurate and repeatable measurements) at five different points on the exterior surface of the slab. The average of these readings was used to determine the rooftop temperature. The accuracy of measurement lies within ±1.5% error, which can be considered highly accurate. Similarly, the roof bottom surface temperature was recorded at the central point of the interior slab surface. Internal air temperature was estimated by holding a matte paper target at multiple positions (centre and corners) inside the test room, allowing thermal equilibrium with the surrounding air and recording its surface temperature using the infrared (IR) thermometer.

The average of these measurements was considered the room air temperature. This method was suitable due to the small volume (1 m^3) and minimal air stratification within the space. The various types of roof slabs used in this experiment are given in Table 1.

Figure 1 shows a roof slab with dry coconut shell. Above the 100 mm RCC slab, chiselled 25 mm inverted dry coconut shells were placed. The gaps were filled with asbestos paste to hold it properly. A weatherproof coarse ferrocement slab of 12.5 mm thickness, comprised of steel mesh of 10 mm square size (3 numbers) cast with rich cement mortar (1:2), was placed above the coconut shells.

Fig. 1. Coconut shell roof slab model.

Table 1. Roof slab types and insulating materials.

No.	Roof slab type	Insulating material	λ (W/m K)	U (W/m²K)	Layers
1	Coconut shell	Dry coconut shell	0.164	3.62	100 mm RCC slab; 25 mm inverted dry coconut shell; 12.5 mm ferrocement slab
2	Glass fiber	Fiberglass	0.050	1.60	100 mm RCC slab; 25 mm glass fibre; 12.5 mm ferrocement slab
3	Earthen pots	Earthen pots	0.380	5.28	100 mm RCC slab; 25 mm inverted dry earthen pots; 12.5 mm ferrocement slab
4	Rice husk	Rice husks	0.0727	2.14	100 mm RCC slab; 25 mm rice husk; 12.5 mm ferrocement slab
5	Rubber sheet	Rubber sheet	0.200	2.66	100 mm RCC slab, 17 mm air gap; 8 mm thick rubber sheet; 12.5 mm ferrocement slab
6	Asbestos sheets	Asbestos sheets	0.147	3.40	100 mm RCC slab; 25 mm asbestos sheets; 12.5 mm ferrocement slab
7	Jhama bricks	Jhama brick bats	0.103	2.73	100 mm RCC slab; 25 mm Jhama brick bats; 12.5 mm ferrocement slab
8	Fly ash	Fly ash	0.0856	2.41	100 mm RCC slab; 25 mm fly ash; 12.5 mm ferrocement slab

The trapped air inside the inverted coconut shell acts as a very good insulator. A ferrocement slab is used above the dry inverted coconut shell to make the roof strong and safe. Similarly, the roof slab with other insulating materials is shown in Figs. 2 to 8.

The thermal conductivity of different insulating materials was measured according to ASTM E1530, using the guarded heat flow meter technique (Figs. 9 and 10). The sample of the insulating material was prepared and placed between two surfaces, which are maintained at different temperatures. The schematic diagram of the setup for measuring the thermal conductivity of a test sample is shown in Fig. 9. Fourier's law of heat con-

Fig. 2. Glass fibre roof slab model.

Fig. 3. Earthen pot roof slab model.

Fig. 4. Rice husk roof slab model.

Fig. 5. Rubber sheet roof slab.

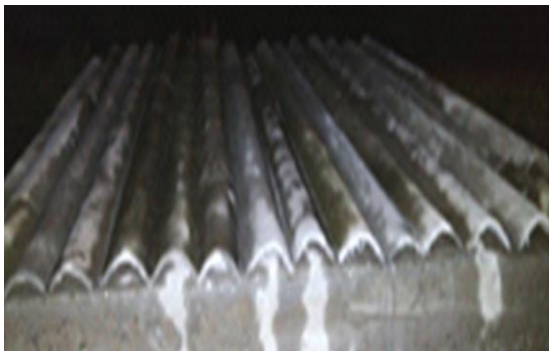

Fig. 6. Roof slab with asbestos sheet.

Fig. 7. Roof slab with Jhama brick bats.

Fig. 8. Fly ash roof slab.

duction was used to determine the thermal conductivity of the test specimen by measuring the temperature difference and the output of the heat flux transducer. From the Fourier law of heat transfer, we have

$$R_s = \frac{T_u - T_m}{Q} - R_{int}, \tag{1}$$

where: R_s − thermal resistance of the test specimen, T_u − temperature of the upper plate, T_m − temperature of the lower plate, Q − heat flux, R_{int} − total interface resistance.

The thermal resistance of the test specimen is given by

$$R_s = \frac{d}{\lambda}, \tag{2}$$

where: d − thickness of the test specimen, λ − thermal conductivity.

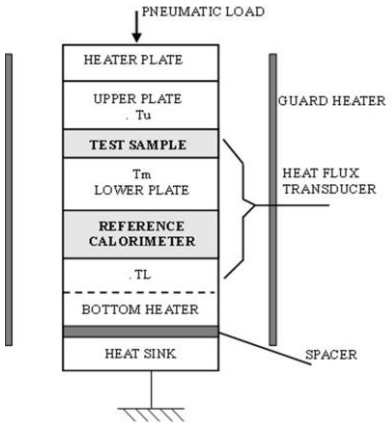

Fig. 9. Diagram of the test section for measuring thermal conductivity.

Fig. 10. Measurement of thermal conductivity according to ASTM E1530. Image courtesy: CIPET, Bhubaneswar.

The interface thermal resistance is considered in Eq. (1) because the temperature difference is measured between the upper and lower surface plates.

The heat flux is measured by calculating the temperature across the reference calorimeter:

$$Q = N(T_m - T_l), \tag{3}$$

where: N – heat transfer coefficient of the reference calorimeter, T_m – surface temperature of the lower plate, T_l – temperature of the bottom heater.

Combining Eqs. (1) and (3), we can find the thermal resistance of the test sample:

$$R_s = F\frac{T_u - T_m}{T_m - T_l} - R_{int}$$

or (4)

$$R_s = F\frac{\Delta T_s}{\Delta T_r} - R_{int},$$

where: $F - 1/N$, ΔT_s – temperature difference across the sample, ΔT_r – temperature difference across the reference calorimeter.

Under ideal conditions, at steady state, the factor F is inversely proportional to the heat transfer coefficient (N) of the reference calorimeter. Such conditions are closely approximated in the method because a guard heater surrounds the test stack. The thermal conductivity measurement device (Model 2022) is calibrated to find F and R_{int}. From Eq. (4), it yields that there is a straight-line relationship between variables R_s and $\Delta T_s/\Delta T_r$. Temperatures are measured to determine the ΔT ratio for several samples, whose thermal resistances are known. These are plotted on a graph to get a straight line, as shown in Fig. 11. The slope of this line gives F, and the ordinate axis intercept is R_{int}. Points A through D represent various calibration samples. Once the relationship between R_s and the ΔT ratio is known, following the equipment calibration, the thermal resistance of any unknown sample can be readily obtained after measuring the temperatures during the test and then calculating the ΔT ratio, as shown by the dotted lines in Fig. 11. For the test result to be accurate, the thermal resistance thus obtained must fall within the range of the samples used during calibration. Once the thermal resistance has been determined, thermal conductivity can be computed from Eq. (2).

3. Results and discussion

This study is fully based on real-time investigation under open environmental conditions. The performance of nine roof slabs (eight with insulation and one without insulation) is calculated based on atmospheric temperatures at various time periods. Correspondingly, the sample thermal conductivity, sample thermal resistivity and the mean sample temperature are computed for

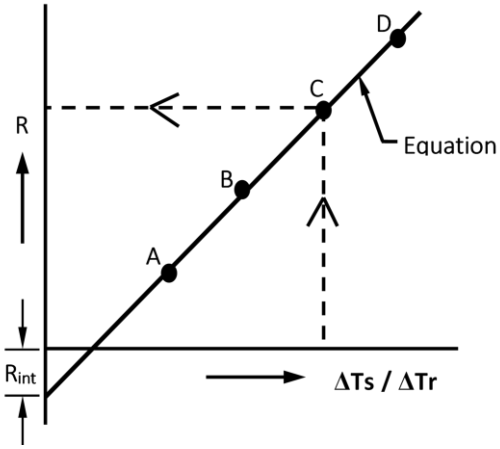

Fig. 11. Equipment calibration and data analysis.

roof sections with and without insulating materials.

The data taken from the real-time analysis were implemented in the MATLAB software.

For each case studied, the temperature between 7.30 am and 10.00 pm was analysed. The average temperature at the roof top, roof bottom and in the room was measured for the roof slab with and without insulating materials to eventually demonstrate the effect of insulating material on the room temperature.

3.1. Performance characteristics of roof slab with inverted coconut shell and the global optimisation techniques

Figure 12 illustrates the thermal performance of the roof slab with inverted coconut shells as insulating material. At 2.30 pm, the temperature of the rooftop reached the peak value, and thereafter the temperature gradually decreased. It is evident from the graph that the temperature of the rooftop with insulation attains the maximum value of 59.45°C at 2.30 pm, whereas the temperature of the roof bottom attains the maximum value of 38.76°C at 4.30 pm. The temperature of the room without insulation attains a maximum value of 41.52°C at 4.00 pm, whereas the temperature of the room with insulation attains a maximum value of 38.58°C at 5.00 pm. Thus, there is a decrease in temperature of the room for the roof slab with insulation by 2.94°C with a time lag of 1.00 h. The time lag between the maximum rooftop temperature and the maximum room temperature is 2.30 h.

A comparison of actual values of the roof bottom temperature with those predicted by five optimisation techniques considered in this study is shown in Table 2. The data clearly indicates that the social spider optimisation (SSO) technique provides the most accurate prediction of temperature values, with the error between the measured and predicted values ranging from 0.12 to 0.91. In comparison, the cuckoo search (CS) optimisation technique yields an error range of 1.38 to 7.92, bacterial colony optimisation (BCO) shows an error between 0.69 and 4.62, group search optimisation (GSO) results in an error of 0.21 to 3.67, and the genetic algorithm (GA) gives an error range of 2.11 to 3.32. Among all these techniques, SSO demonstrates the minimum error, highlighting its superior performance and accuracy in temperature predictions.

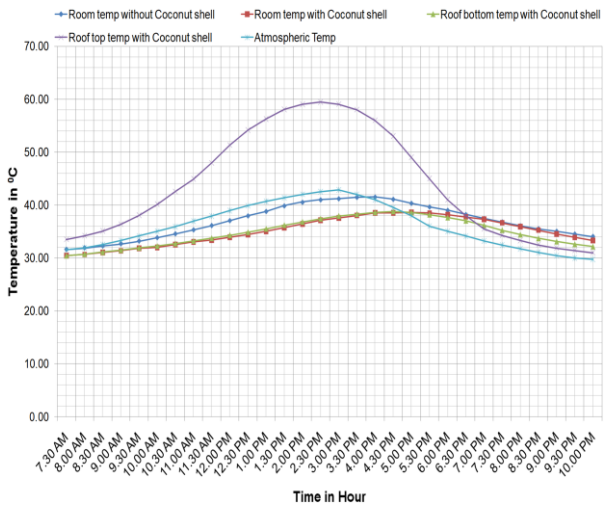

Fig. 12. Real-time performance of the roof slab with coconut shell.

Table 2. Performance characteristics of the roof slab with coconut shell.

Input		Output (temperature, °C)						
				Predicted value				
Area, m²	Thickness, m	Testing temperature (roof top)	Actual value (roof bottom)	SSO	GA	GSO	CS	BCO
1	0.1397	33.50	30.45	30.57	32.56	30.67	31.83	31.14
		34.20	30.75	30.91	33.35	30.99	32.2	31.44
		35.10	31.11	31.29	34.02	31.32	33.35	31.83
		36.36	31.49	31.61	34.65	31.72	33.75	32.26
		38.05	31.92	32.13	35.11	32.2	34.26	32.79
		40.15	32.27	32.52	35.49	32.58	34.81	33.16
		42.52	32.74	33.02	36.03	33.09	35.98	33.92
		44.92	33.22	33.54	36.54	33.63	37.06	34.51
		47.92	33.73	34.1	36.83	34.54	37.87	35.59
		51.32	34.3	34.71	37.28	35.71	38.64	36.19
		54.15	34.87	35.34	37.59	35.99	39.63	36.97
		56.24	35.5	36.03	38.14	36.62	40.42	37.66
		58.05	36.19	36.77	38.81	38.31	41.32	38.38
		58.98	36.8	37.4	39.39	38.99	42.07	39.03
		59.45	37.4	37.52	39.94	40.52	42.78	39.66
		59.05	37.92	38.55	40.43	41.16	43.71	41.06
		58.00	38.25	38.94	40.72	41.92	44.19	41.54
		56.00	38.58	39.29	41.02	41.76	44.72	40.77
		53.00	38.76	39.5	41.17	41.94	45.43	42.94
		49.00	38.55	39.33	40.94	41.53	45.67	42.84
		45.00	38.15	39.06	40.47	40.99	45.52	42.77
		41.00	37.6	38.38	39.9	40.78	45.24	40.86
		38.00	37	37.74	39.26	39.18	44.91	40.24
		35.50	36.15	36.86	38.38	38.27	44.09	39.42
		34.30	35.25	35.93	37.35	37.33	36.67	37.48
		33.30	34.4	35.01	36.79	35.58	41.93	36.59
		32.50	33.7	34.27	36.02	34.84	39.84	35.81
		31.90	33.1	33.64	35.4	34.18	39.1	35.08
		31.40	32.6	33.11	34.86	33.59	37.94	33.87
		31.00	32.15	32.55	34.38	32.83	36.53	32.92

3.2. Performance characteristics of roof slab with fibreglass and the global optimisation techniques

Figure 13 visualises the real-time thermal performance of the roof slab with glass fibre. It can be observed from the figure that the temperature of the roof bottom with insulation attains the maximum value of 35.58°C at 6.00 pm, whereas the temperature of the room attains a maximum value of 35.35°C at 6.30 pm.

Thus, compared to the non-insulated roof slab case (peak room temperature of 41.52°C at 4.00 pm), there is a decrease in temperature of the room for the roof slab with insulation by

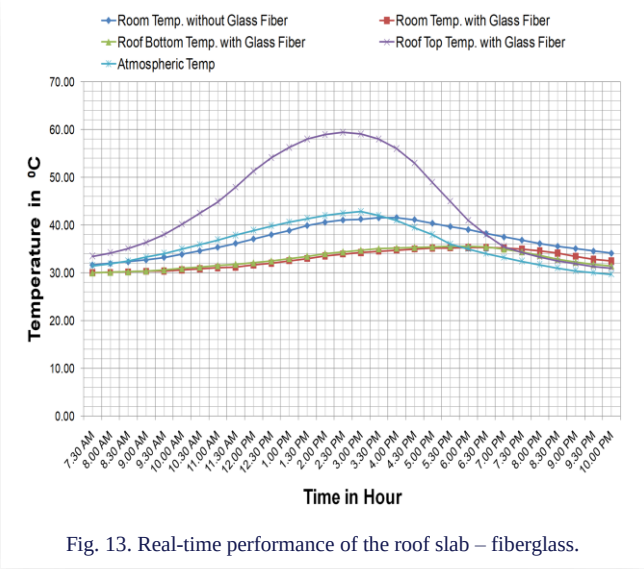

Fig. 13. Real-time performance of the roof slab – fiberglass.

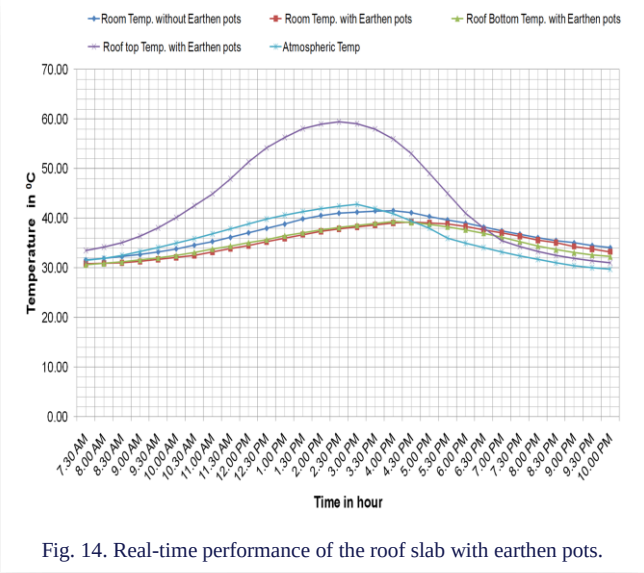

Fig. 14. Real-time performance of the roof slab with earthen pots.

6.17°C with a time lag of 2.30 h. The time lag between the maximum rooftop temperature and the maximum room temperature is 4.00 h. Since the coefficient of emissivity of the fibreglass varies between 0.85 to 0.95 and the thermal conductivity is 0.05 W/(m K), the temperature of the room is reduced by the maximum amount.

Similarly, among the optimisation techniques used, in this case, SSO was found to demonstrate the highest accuracy, with an error range of 0.08–0.99 between measured and predicted temperatures. GSO also gave good predictions, with an error range of 0.16–4.32, followed by BCO (0.97–7.07), GA (2.10–3.30) and CS (1.34–9.34). These results show that the SSO method provides the most reliable predictions, significantly reducing the error margin compared to other optimisation methods. It was observed that the SSO technique predicts the temperature accurately, and the error between the measured and predicted value of temperature is minimum.

The fibreglass layer, encapsulated beneath a 12.5 mm thick ferrocement slab, reduces indoor temperature primarily due to its low thermal conductivity (0.05 W/(m·K)), which significantly impedes heat transfer through the roof. The emissivity of fibreglass does not directly affect the heat exchange process in this configuration, as it is not exposed to external radiation.

3.3. Performance characteristics of the roof slab with earthen pots and the global optimisation techniques

Figure 14 depicts the real-time thermal performance of a roof slab with earthen pots. While the temperature of the rooftop with insulation attains the maximum value of 59.45°C at 2.30 pm, the temperature of the roof bottom in this case attains the maximum value of 39.35°C at 4.00 pm, and the temperature of the room reaches a maximum value of 39.25°C at 4.30 pm. Thus, there is a decrease in temperature of the room for the roof slab with insulation by 2.27°C compared to a roof without insulation, with a time lag of 0.30 h. The time lag between the maximum rooftop temperature and the maximum room temperature is 2.00 h. The roof bottom temperature was predicted using five optimisation techniques, such as cuckoo search, bacterial colony optimisation, group search optimisation, genetic algorithm, and social spider optimisation. The error range between the measured and predicted values for various optimisation methods is: CS (1.37–7.99), BCO (0.67–4.54), GSO (0.16–3.33), GA (2.10–3.30), and SSO (0.12–0.82). Among these, the SSO technique exhibited the highest accuracy, with the minimum error range, indicating its superior performance in precisely envisaging the roof bottom temperature.

3.4. Performance characteristics of roof slab with rice husk and the global optimisation techniques

The real-time performance of the roof slab with rice husk is displayed in Fig. 15. The results reveal that the temperature of the roof bottom with insulation attains the maximum value of 36.88°C at 5.30 pm, whereas the temperature of the room attains a maximum value of 36.70°C at 6.00 pm. A decrease in

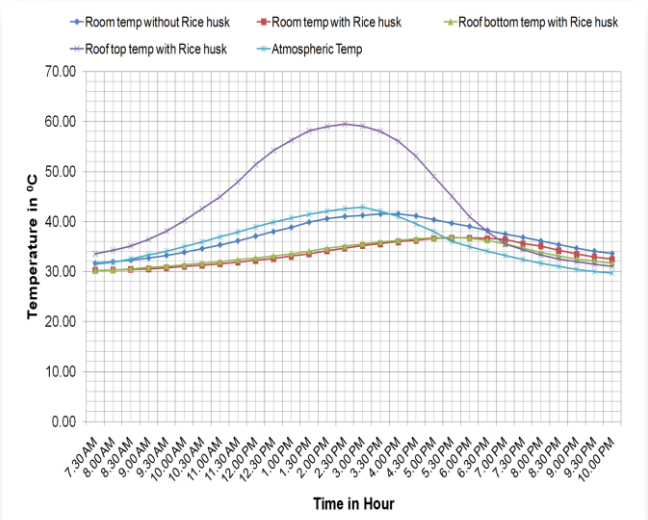

Fig. 15. Real-time performance of the roof slab with rice husk.

the room temperature for the roof slab with insulation compared to a roof without insulation is 4.82°C with a time lag of 2.00 h. The time lag between the maximum rooftop temperature and the maximum room temperature is 3.30 h.

The error ranges for different optimisation methods were CS (1.34–8.14), BCO (0.67–4.54), GSO (0.16–3.30), GA (2.10–3.30) and SSO (0.12–0.82). This shows that, also in this case, SSO exhibited the highest accuracy with the lowest prediction error.

3.5. Performance characteristics of roof slab with rubber sheets and the global optimisation techniques

Figure 16 demonstrates the real-time thermal performance of the roof slab with rubber sheets as an insulating material.

The results show that the temperature of the roof bottom with this insulation type reaches the maximum value of 39.18°C at 4.00 pm, while the maximum room temperature of 39.05°C is reached at 4.30 pm. Considering that the room temperature without insulation attains a maximum value of 41.52°C at 4.00 pm, there is a decrease in temperature of the room for the roof slab with insulation by 2.47°C with a time lag of 0.30 h. The time lag between the maximum rooftop temperature and the maximum room temperature is 2.00 h.

Temperature prediction errors using five optimisation methods were as follows: CS (1.46–7.91), BCO (0.32–2.11), GSO (0.67–4.29), GA (2.10–3.30) and SSO (0.12–0.78). Among all these methods, SSO demonstrated the highest accuracy with the lowest error, indicating its superior performance compared to CS, BCO, GSO and GA.

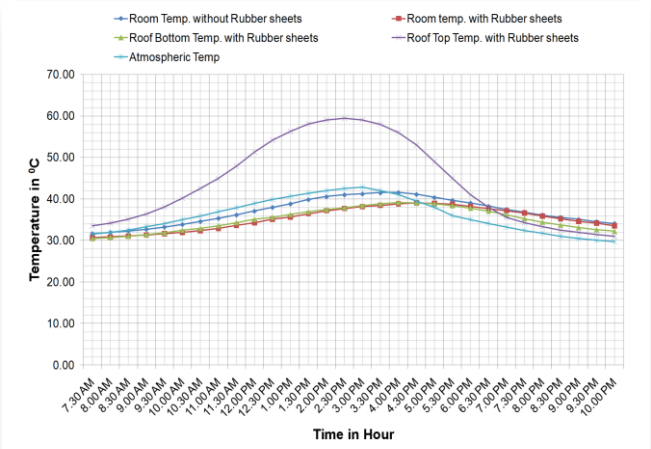

Fig. 16. Real-time performance of the roof slab – rubber sheets.

3.6. Performance characteristics of roof slab with asbestos sheet and the global optimisation techniques

Figure 17 shows the real-time thermal performance of the roof slab with an asbestos sheet. As can be seen from the figure, the temperature of the roof bottom attains a maximum of 38.33°C at 5.00 pm.

A comparison of the temperature in a room for the case of roof without insulation (a peak value of 41.52°C at 4.00 pm)

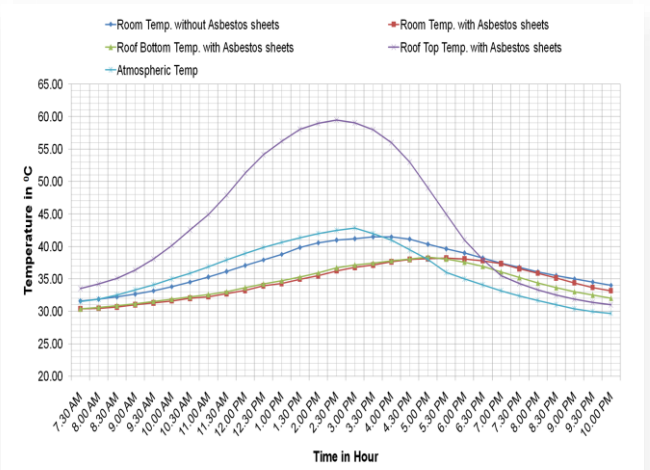

Fig. 17. Real-time performance of the roof slab with asbestos sheet.

with the one for the insulated roof case that reaches a peak value of 38.22°C at 5.30 pm, indicates that there is a decrease in temperature of the room for the roof slab with insulation by 3.30°C with a time lag of 1.30 h. The time lag between the maximum rooftop temperature and the maximum room temperature with insulation is 3.00 h.

The error ranges between measured and predicted roof bottom temperatures for different optimisation methods were as follows: 1.37–8.14 for the cuckoo search, 0.67–4.54 for the bacterial colony optimisation, 2.10–3.30 for the genetic algorithm, 0.16–3.30 for the group search optimisation and 0.12–0.82 for the social spider optimisation. Out of these five optimisation techniques, SSO was found to be the most effective technique with the highest prediction accuracy.

3.7. Performance characteristics of roof slab with Jhama brick bats and the global optimisation techniques

The real-time thermal performance of the roof slab with Jhama brick bats as insulating material is presented in Fig. 18. The measured average temperatures at the roof top, roof bottom and in the room for the insulated roof slab were compared with the corresponding temperatures for the roof slab without insulation. In this case, the maximum temperature of the roof bottom with insulation, amounting to 38.21°C, is achieved at 5.00 pm, whereas the temperature of the room attains a maximum value of 38.05°C at 5.30 pm. Since the room temperature in the case of a non-insulated roof slab reaches a maximum value of 41.52°C at 4.00 pm, it follows that there is a decrease in temperature of the room for the roof slab with insulation by 3.47°C with a time lag of 1.30 h. The time lag between the maximum rooftop temperature and the maximum room temperature is 3.00 h.

The prediction errors between measured and estimated roof bottom temperatures using various optimisation techniques were as follows: 1.34–8.14 for the cuckoo search technique, 0.67–4.54 for the bacterial colony optimisation, 2.10–3.30 for the genetic algorithm, 0.16–3.30 for the group search optimisation and 0.12–0.79 for the social spider optimisation. Similarly, it is concluded that SSO demonstrated the highest accuracy, characterised by the lowest error range. A comparative analysis

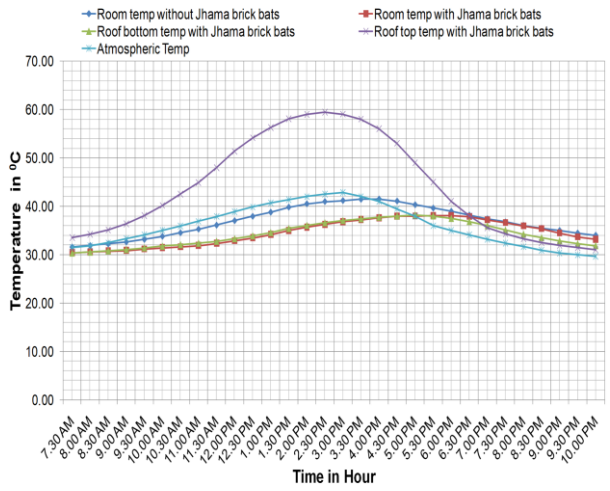

Fig. 18. Real-time performance of the roof slab – Jhama brick bats.

confirms that SSO outperforms the other four techniques in predicting temperature with greater accuracy.

3.8. Performance characteristics of roof slab with fly ash and the global optimisation techniques

Figure 19 demonstrates the real-time thermal performance of the roof slab with fly ash as an insulating material. While the temperature of the rooftop with insulation attains its maximum of 59.45°C at 2.30 pm, the peak temperature of the roof bottom in this case is 37.20°C and is reached at 5.30 pm. The room temperature reaches a maximum value of 37.08°C at 6.00 pm, which is a decrease of 4.44°C compared to the non-insulated roof case, with a time lag of 2.00 h. The time lag between the maximum rooftop temperature and the maximum room temperature is 3.30 h.

The error ranges between the measured and predicted roof bottom temperatures using various optimisation methods were as follows: 1.34–8.14 for the cuckoo search method, 0.67–4.54 for the bacterial colony optimisation, 2.10–3.30 for the genetic algorithm, 0.16–3.30 for the group search optimisation and 0.12–0.82 for the social spider optimisation. Among all the

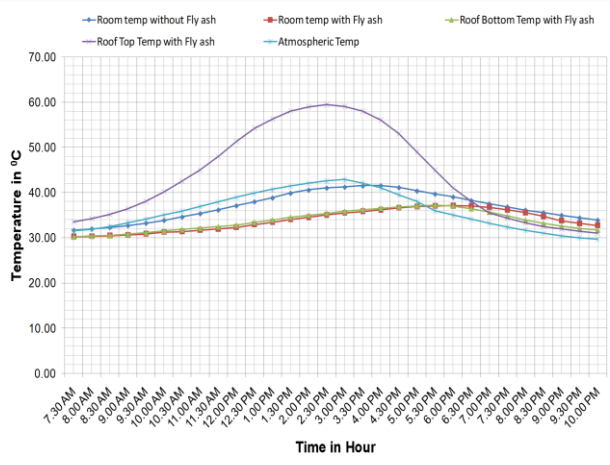

Fig. 19. Real-time performance of the roof slab – fly ash.

methods considered, SSO exhibited the highest accuracy, yielding the lowest prediction error, which confirms that SSO outperforms the other four algorithms in temperature prediction accuracy.

3.9. Performance characteristics of roof slab without insulating material and the global optimisation techniques

Figure 20 demonstrates the real-time thermal performance of the roof slab without insulation, including recorded average temperatures at the roof top, roof bottom and inside the room. The rooftop temperature reached its peak (59.45°C) at 2:30 pm and thereafter gradually decreased, whereas the temperature of the roof bottom attained the maximum value of 41.75°C at 3.30 pm. The maximum temperature in the room was 41.52°C and was obtained at 4.00 pm. The time lag between the maximum rooftop temperature and the maximum room temperature is 1.30 h.

Similarly, the variation in roof bottom temperature was predicted using five optimisation techniques – bacterial colony optimisation (BCO), social spider optimisation (SSO), group search optimisation (GSO), cuckoo search (GS) and genetic algorithm (GA), and the results were compared with actual values. The error ranges for different optimisation methods were: CS (1.37–7.95), BCO (0.69–4.36), GA (2.18–3.29), GSO (0.19–3.28) and SSO (0.12–0.96).

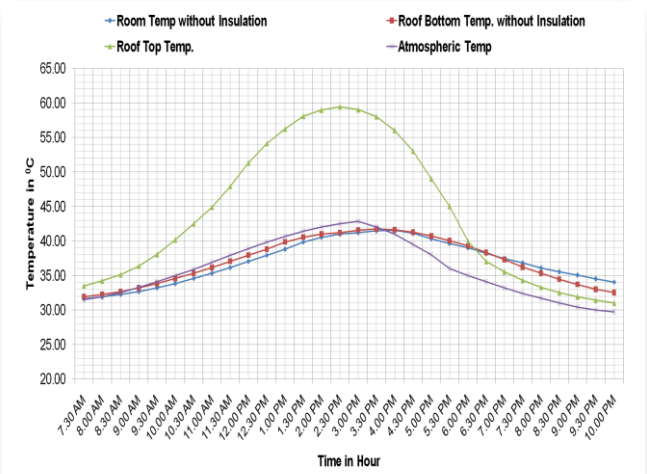

Fig. 20. Real-time performance of the roof slab without insulating material.

Out of five optimisation techniques considered, SSO was found to exhibit the highest accuracy with the lowest prediction error, thus confirming its superior performance compared to the other four methods. The effect of all the insulating materials, considered in this study, on the room temperature is plotted in Fig. 21. The performance of roof slabs with various insulating materials is summarised in Table 3. The time lag between the maximum room temperature with and without insulation is found to be maximum in case of glass fibre and minimum in the case of earthen pots. Similarly, the maximum reduction in room temperature with roof slab insulation was found to be 6.17°C in the case of glass fibre and 2.27°C in the case of earthen pots.

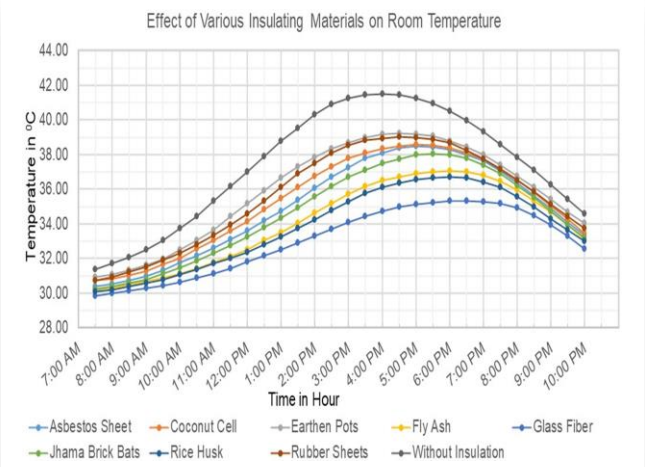

Fig. 21. Effect of various insulating materials on the room temperature.

Table 3. Comparison of the roof slab thermal performance with and without different insulation materials.

No.	Insulation material	Roof top temp., °C / time	Room temp. with insulation, °C / time	Room temp. without insulation, °C / time	Temp. reduction in the room, °C	Time lag (room vs. no insulation)	Time lag, h (roof top vs. room)
1	Inverted coconut shell	59.45 / 2:30 pm	38.58 / 5:00 pm	41.52 / 4:00 pm	2.94	1.00	2.30
2	Glass fibre	59.45 / 2:30 pm	35.35 / 6:30 pm	41.52 / 4:00 pm	6.17	2.30	4.00
3	Earthen pots	59.45 / 2:30 pm	39.25 / 4:30 pm	41.52 / 4:00 pm	2.27	0.30	2.00
4	Rice husk	59.45 / 2:30 pm	36.70 / 6:00 pm	41.52 / 4:00 pm	4.82	2.00	3.30
5	Rubber sheets	59.45 / 2:30 pm	39.05 / 4:30 pm	41.52 / 4:00 pm	2.47	0.30	2.00
6	Asbestos sheet	59.45 / 2:30 pm	38.22 / 5:30 pm	41.52 / 4:00 pm	3.30	1.30	3.00
7	Jhama brick bats	59.45 / 2:30 pm	38.05 / 5:30 pm	41.52 / 4:00 pm	3.47	1.30	3.00
8	Fly ash	59.45 / 2:30 pm	37.08 / 6:00 pm	41.52 / 4:00 pm	4.44	2.00	3.30
9	No insulation	59.45 / 2:30 pm	—	41.52 / 4:00 pm	—	—	1.30

The experimental analysis clearly demonstrates that the inclusion of insulating materials on roof slabs leads to a significant reduction in indoor temperature and delays the thermal response of the indoor environment. The most striking finding is the superior performance of fibreglass, which not only achieved the highest temperature reduction (6.17°C) but also the longest time lag (4 h). This is attributable to its low thermal conductivity 0.05 W/(m·K), which significantly impedes heat transfer through the roof.

In contrast, natural and waste-based materials such as coconut shells, rice husks and Jhama brick bats also demonstrated appreciable performance, with temperature reductions ranging between 2.94°C and 4.82°C. These materials are highly porous, contain trapped air pockets and have relatively low thermal conductivities, making them effective as low-cost, sustainable insulators.

The time lag is a particularly important metric from a comfort and energy efficiency standpoint. For example, a delay of 2–4 hours in peak room temperature relative to peak rooftop temperature helps reduce the HVAC system loads during the hottest part of the day. This could translate to significant energy savings, particularly in tropical and subtropical regions.

Materials like earthen pots and rubber sheets, though less effective than fibreglass or rice husk, still provided substantial benefits. The relatively lower performance may be due to factors like higher density (in the case of earthen pots) or limited thickness and air gap arrangement (in rubber sheets), which reduce their insulation capacity.

The prediction models using metaheuristic optimisation methods further reinforce the experimental observations. The fact that the social spider optimisation consistently achieved the lowest error margins highlights the potential of such techniques in predicting thermal behaviour and reducing the dependency on exhaustive experimental trials. Moreover, the experimental setup using identical test rooms and real outdoor conditions adds practical relevance to the findings. Unlike simulation-only studies, this real-world data offers actionable insights for architects, builders and policy-makers seeking passive solutions for thermal management in buildings.

4. Conclusions

The thermal performances of eight roof slabs with insulating materials were compared with the roof slab without an insulating material under the same atmospheric conditions. Eight insulating materials such as coconut shell, fibreglass, fly ash, rubber sheet, asbestos sheets, rice husk, Jhama brick bats and earthen pots were utilised in this study. The variation of the roof bottom temperature was predicted using five optimisation techniques, such as bacterial colony optimisation, group search optimisation, cuckoo search, genetic algorithm and social spider optimisation. Based on the experimental test results and theoretical analysis, the following conclusions have been drawn:

(i) The time difference between the peak external (roof top) temperature and the corresponding peak internal (room) temperature was recorded for each type of insulation. This metric indicates the material's ability to delay heat penetration, which is critical for maintaining thermal comfort during peak summer hours. For example, the fibreglass roof showed a maximum time lag of 4 h, while the earthen pot roof showed a minimum lag of 2 h.

(ii) The difference in indoor temperature between rooms with and without insulation was quantified. This reduction reflects the insulator's ability to mitigate indoor heat gain. Fibreglass achieved a reduction of 6.17°C, whereas for earthen pots it was 2.27°C.

(iii) Using the ASTM E1530 guarded heat flow meter method, the thermal conductivity of each insulating material was experimentally determined. Corresponding thermal resistance values were calculated using Fourier's

law. These provide direct insight into the heat transfer inhibition through each material.

(iv) The overall heat transfer coefficient was computed for each roof slab configuration, reflecting the heat transfer rate through the composite slab. A lower overall heat transfer coefficient indicates better insulation.

(v) The study applied five metaheuristic algorithms to predict roof bottom temperatures, comparing them to actual experimental data. The error range between predicted and measured values served as a performance indicator of both insulation efficiency and the robustness of modelling methods. Social spider optimisation demonstrated the highest level of accuracy in prediction, with errors as low as 0.08°C.

(vi) While the actual energy expenditure (e.g. cooling load or kilowatt-hours saved) was not measured directly, temperature reduction and time lag can be used as alternative metrics. These reductions are directly correlated with decreased energy demands for ventilation and air conditioning. Thus, the findings support energy-saving implications for passive cooling strategies.

(vii) It was observed that the social spider optimisation technique predicted the roof bottom temperature accurately, and the error between the measured and predicted value of temperature was minimum as compared to the other four optimisation techniques.

(viii) The performance of the roof slab using different insulating materials in descending order is found to be fibreglass, rice husk, fly ash, Jhama brick bats, asbestos sheet, coconut shell, rubber sheet and earthen pot.

References

[1] Rajeev, P., Sanjayan, J.G., & Seenuth, S.S. (2016): Assessment of thermal cracking in concrete roof tiles. *Journal of Materials & Design*, 107, 470–477. doi: 10.1016/j.matdes.2016.06.072

[2] Al-Sanea, S.A. (2002). Thermal performance of building roof elements. *Journal of Building and Environment*, 37(7), 665–675. doi: 10.1016/S0360-1323(01)00077-4

[3] Zhang, Z., Tong, S., & Yu, H. (2016). Life Cycle Analysis of Cool Roof in Tropical Areas. *Procedia Engineering*, 169, 392–399. doi: 10.1016/j.proeng.2016.10.048

[4] Venugopal, P.R., Murugan, R., Thyla, P.R., Aithal, S., Babu, R., Perumal, C., & Raj, V.B. (2015). Experimental and numerical investigations on roof slab of a pool type sodium cooled fast reactor based on model studies. *Annals of Nuclear Energy*, 85, 1085–1095. doi: 10.1016/j.anucene.2015.06.045

[5] Ramamurthy, P., Sun, T., Rule, K., & Bou-Zeid, E. (2015). The joint influence of albedo and insulation on roof performance. A modeling study. *Energy and Buildings*, 102, 317–327 doi: 10.1016/j.enbuild.2015.06.005

[6] Lundholm, T.J., Weddle, B.M., & Maclvor, J.S. (2014). Snow depth and vegetation type affect green roof thermal performance in winter. *Energy and Buildings*, 84, 299–307. doi: 10.1016/j.enbuild.2014.07.093

[7] Kumar, A., & Suman, B.M. (2013). Experimental evaluation of insulation materials for walls and roofs and their impact on indoor thermal comfort under composite climate. *Building and Environment*, 59, 635–643. doi: 10.1016/j.buildenv.2012.09.023

[8] Jim, C.Y. (2014). Air-conditioning energy consumption due to green roofs with different building thermal insulation. *Applied Energy*, 128, 49–59. doi: 10.1016/j.apenergy.2014.04.055

[9] Berardi, U., & Naldi, M. (2017). The impact of the temperature dependent thermal conductivity of insulating materials on the effective building envelope performance. *Energy and Buildings*, 144, 262–275 doi: 10.1016/j.enbuild.2017.03.052

[10] D'Orazioa, M.D., Perna, C.D., & Giuseppe, E.D. (2010): The effects of roof covering on the thermal performance of highly insulated roofs in Mediterranean climates. *Energy and Buildings*, 42(10), 1619–1627. doi: 10.1016/j.enbuild.2010.04.004

[11] Björk, F., & Enochsson, T. (2009). Properties of thermal insulation materials during extreme environment changes. *Construction and Building Materials*, 23(6), 2189–2195. doi: 10.1016/j.conbuildmat.2008.12.006

[12] Gagliano, A., Patania, F., Nocera, F., Ferlito, A., & Galesi, A. (2012). Thermal performance of ventilated roofs during summer period. *Energy and Buildings*, 49, 611–618 doi: 10.1016/j.enbuild.2012.03.007

[13] Halwatura, R.U., & Jayasinghe, M.T.R. (2008). Thermal performance of insulated roof slabs in tropical climates. *Energy and Buildings*, 40(7), 1153–1160. doi: 10.1016/j.enbuild.2007.10.006

[14] Jaffal, I., Ouldboukhitine, S.-E., & Belarbi, R. (2012). A comprehensive study of the impact of green roofs on building energy performance. *Renewable Energy*, 43, 157–164. doi: 10.1016/j.renene.2011.12.004

[15] Dong, L., Yumeng, Z., Changyu, L., & Guozhong, W. (2015). Numerical analysis on thermal performance of roof contained PCM of a single residential building. *Energy Conversion and Management*, 100, 147–156. doi: 10.1016/j.enconman.2015.05.014

[16] Dixit, A.K., Roul, M.K., & Panda, B.C. (2017). Designing an efficient mathematical model for different thermal insulation material using group search optimization. *International Journal of Intelligent Engineering and Systems*, 10(1), 28–37. doi: 10.22266/ijies2017.0228.04

[17] Dixit, A.K., Roul, M.K., & Panda, B.C. (2019). Mathematical model using soft computing techniques for different thermal insulation materials. *Journal of Intelligent Systems*, 28(5), 821–833. doi: 10.1515/jisys-2017-0103

[18] Dixit, A.K., Roul, M.K., & Panda, B.C. (2018). Numerical techniques for different thermal insulation materials. *International Journal of Optimization in Civil Engineering*, 8(1), 29–42. doi: joce.iust.ac.ir/article-1-323-en

[19] Roul, M.K., & Nayak, R.C. (2012). Experimental investigation of natural convection heat transfer through heated vertical tubes. *International Journal of Engineering Research and Applications*, 2(6), 1088–1096.

[20] Nayak, R.C., Roul, M.K., & Sarangi, S.K. (2017). Experimental investigation of natural convection heat transfer in heated vertical tubes with discrete rings. *Experimental Techniques*, 41, 585–603. doi: 10.1007/s40799-017-0201-6

[21] Nayak, R.C., Roul, M.K., & Sarangi, S.K. (2017). Experimental investigation of natural convection heat transfer in heated vertical tubes. *International Journal of Applied Engineering Research*, 12(10), 2538–2550.

[22] Nayak, R.C., Roul, M.K., & Sarangi, S.K. (2018). Natural convection heat transfer in heated vertical tubes with internal rings. *Archives of Thermodynamics*, 39(4), 85–111. doi: 10.1515/aoter-2018-0031

[23] Sahoo, L.K., Roul, M.K., & Swain, R.K., (2017). CFD analysis of steady laminar natural convection heat transfer from a pin

finned isothermal vertical plate. *Heat Transfer—Asian Research*, 46(7), 840–862. doi: 10.1002/htj.21246

[24] Sahoo, L.K., Roul, M.K., & Swain, R.K. (2017). Natural convection heat transfer augmentation factor with square conductive pin fin arrays. *Journal of Applied Mechanics and Technical Physics*, 58, 1115–1122. doi: 10.1134/S0021894417060189

[25] Sahoo, L.K., Roul, M.K., & Swain, R.K. (2018). CFD analysis of natural convection heat transfer augmentation from square conductive horizontal and inclined pin fin arrays. *International Journal of Ambient Energy*, 39(8), 840–851. doi: 10.1080/01430750.2017.1354317

[26] Sahoo, L.K., Roul, M.K., & Swain, R.K. (2017). CFD analysis of heat transfer in hexagonal subchannels of super-fast reactor in upward flow. *Heat Transfer—Asian Research*, 46(8), 1399–1412. doi: 10.1002/htj.21281

[27] Roul, M.K., & Sahoo, L.K. (2012). CFD modeling of pressure drop caused by two-phase flow of oil/water emulsions through sudden expansions. *International Journal of Engineering Research and Applications*, 2(6), 1047–1054.

[28] Himrane, N., Ameziani, D.E., & Nasseri, L. (2020). Study of thermal comfort: numerical simulation in a closed cavity using the lattice Boltzmann method. *SN Applied Sciences*, 2, 785. doi: 10.1007/s42452-020-2600-z

[29] Belenguer, E., García, N., & Sabater-Grande, G. (2019). Assessment of energy efficiency improvement methods in the residential sector through the development of economic experiments. SN *Applied Sciences*, 1, 1409. doi: 10.1007/s42452-019-1439-7

[30] Martínez, M., Huygen, N., Sanders, J., & Atamturktur, S. (2018). Thermo-fluid dynamic analysis of concrete masonry units via experimental testing and numerical modeling. *Journal of Building Engineering*, 19, 80–90. doi: 10.1016/j.jobe.2018.04.029

[31] Chandra, M.S., Nandapala, K., Priyadarshana, G. & Halwatura, R.U. (2019). Developing a durable thermally insulated roof slab system using bamboo insulation panels. *International Journal of Energy and Environmental Engineering*, 10(4), 511–522. doi: 10.1007/s40095-019-0308-x

[32] Koru, M. (2016). Determination of thermal conductivity of closed-cell insulation materials that depend on temperature and density. *Arabian Journal for Science and Engineering*, 41, 4337–4346. doi: 10.1007/s13369-016-2122-6

[33] Alyami, S.H. (2019). Critical analysis of energy efficiency assessment by international green building rating tools and its effects on local adaptation. *Arabian Journal for Science and Engineering*, 44, 8599–8613. doi: 10.1007/s13369-019-03972-x

[34] Kumar, D., Ali, I., Hakeem, M., Junejo, A., & Harijan, K. (2019). LCC optimization of different insulation materials and energy sources used in HVAC duct applications. *Arabian Journal for Science and Engineering*, 44, 5679–5696. doi: 10.1007/s13369-018-3689-x

[35] Alnahhal, M., Elnaggar, M., &, Edwan, E. (2018). Thermal analysis and thickness optimization of two-cavity thermal insulator in buildings. *Arabian Journal for Science and Engineering*, 43, 1369–1381. doi: 10.1007/s13369-017-2854-y

[36] Alhefnawi, M.A.M., & Abdu-Allah Al-Qahtany, M. (2017). Thermal insulation efficiency of unventilated air-gapped facades in hot climate. *Arabian Journal for Science and Engineering*, 42, 1155–1160. doi: 10.1007/s13369-016-2370-5

[37] Sassine, E., Cherif, Y., Dgheim, J., & Antczak, E. (2020). Experimental and numerical thermal assessment of Lebanese traditional hollow blocks. *International Journal of Thermophysics*, 41, 47. doi: 10.1007/s10765-020-02626-7